Weak Galerkin Finite Element Methods for the Darcy Equation

Zhuoran Wang

Colorado State University

07/05/2017

Master Defense

Acknowledgements

Master's Committee:

- Advisor: Dr. James Liu
- Co-Advisor: Dr. Simon Tavener
- Dr. Tammy Donahue

Funding

- National Science Foundation, DMS-1419077
- CSU CIMS Graduate Fellowship Summer 2016

Talk Outline

- Darcy Equation
- Existing Finite Element Methods
  - Continuous Galerkin Finite Element Methods (CGFEMs)
  - Mixed Finite Element Methods (MFEMs)
- Weak Galerkin Finite Element Methods (WGFEMs) for Darcy in 2-dim.
- Weak Galerkin Finite Element Methods for Darcy in 3-dim.
- Weak Galerkin Finite Element Methods for Elasticity

Darcy Equation

Darcy equation usual form:

$$\begin{cases} \nabla \cdot (-\mathbf{K}\nabla p) \equiv \nabla \cdot \mathbf{u} = f, \quad \mathbf{x} \in \Omega, \\ p = p_D, \ \ \mathbf{x} \in \Gamma^D, \qquad \mathbf{u} \cdot \mathbf{n} = u_N, \ \ \mathbf{x} \in \Gamma^N, \end{cases} \tag{1}$$

- p is the unknown pressure
- $\mathbf{K}$ is a permeability tensor, SPD
- f is a source term
- p_D is Dirichlet boundary data
- u_N is Neumann boundary data

For simplicity, let's consider the Darcy equation with homogeneous Dirichlet B.C. on the entire boundary.

CG Finite Element Scheme

Through integration by parts, the **variational form** is

$$\int_\Omega \mathbf{K}\nabla p \cdot \nabla q = \int_\Omega fq,\ \forall q \in V, \tag{2}$$

where Ω is the domain, $V = H_0^1(\Omega)$.

On a subspace $V_h \subset V$, the **CG finite element scheme** is

$$\mathcal{A}_h(p_h, q) = \mathcal{F}(q), \tag{3}$$

where $p_h = \sum_{j=1}^{n} c_j \Phi_j$, q is the test function in the finite element space, $\mathcal{A}_h(p_h, q)$ is the bilinear form

$$\mathcal{A}_h(p_h, q) := \sum_{E \in \mathcal{E}_h} \int_E \mathbf{K}\nabla p_h \cdot \nabla q,\ \forall q \in V_h, \tag{4}$$

$\mathcal{F}(q)$ is the linear form

$$\mathcal{F}(q) := \sum_{E \in \mathcal{E}_h} \int_E f\, q,\ \forall q \in V_h. \tag{5}$$

Features of CGFEMs

- Fewer unknowns compared with MFEMs and WGFEMs,
- Lacks "local mass conservation", that is,

$$\int_E (\nabla \cdot \mathbf{u}) \neq \int_E f,$$

- Lacks "continuity of bulk normal fluxes", that is,

$$\int_\gamma \mathbf{u}_h^{(1)} \cdot \mathbf{n}_1 + \int_\gamma \mathbf{u}_h^{(2)} \cdot \mathbf{n}_2 \neq 0.$$

Mixed Variational Form

Define the Darcy velocity $\mathbf{u} = -(\mathbf{K}\nabla p)$. The second order Darcy can be rewritten as the first order **PDE** system

$$\begin{cases} \mathbf{K}^{-1}\mathbf{u} + \nabla p = 0, & \text{in } \Omega, \\ \nabla \cdot \mathbf{u} = f, & \text{in } \Omega, \end{cases} \tag{6}$$

Mixed Variational Form Seek $\mathbf{u} \in H_{u_N,N}(\mathrm{div}, \Omega)$ and $p \in L^2(\Omega)$ such that

$$\begin{cases} \int_\Omega (\mathbf{K}^{-1}\mathbf{u}) \cdot \mathbf{v} - \int_\Omega p(\nabla \cdot \mathbf{v}) = -\int_{\Gamma_D} p_D \mathbf{v} \cdot \mathbf{n}, & \forall \mathbf{v} \in \mathrm{H}_{0,N}(\mathrm{div}; \Omega), \\ -\int_\Omega (\nabla \cdot \mathbf{u}) q = -\int_\Omega fq, & \forall q \in L^2(\Omega). \end{cases} \tag{7}$$

Mixed finite element scheme Seek $\mathbf{u}_h \in \overline{U}_h$, $p_h \in W_h$ such that

$$\begin{cases} \sum_{E\in\mathcal{E}_h} \int_E (\mathbf{K}^{-1}\mathbf{u}_h) \cdot \mathbf{v} - \sum_{E\in\mathcal{E}_h} \int_E p_h(\nabla \cdot \mathbf{v}) = -\sum_{\gamma\in\Gamma_h^D} \int_\gamma p_D \mathbf{v} \cdot \mathbf{n}, & \forall \mathbf{v} \in U_h^0, \\ -\sum_{E\in\mathcal{E}_h} \int_E (\nabla \cdot \mathbf{u}_h) q = -\sum_{E\in\mathcal{E}_h} \int_E fq, & \forall q \in W_h. \end{cases} \tag{8}$$

Raviart-Thomas (RT) Spaces on Triangles

$RT_0(T)$ for example.

Natural basis

$$RT_0(T) = \text{Span}\left\{\begin{bmatrix} 1 \\ 0 \end{bmatrix}\begin{bmatrix} 0 \\ 1 \end{bmatrix}\begin{bmatrix} x \\ y \end{bmatrix}\right\}. \tag{9}$$

Normalized basis

$$RT_0(T) = \text{Span}\left\{\begin{bmatrix} 1 \\ 0 \end{bmatrix}\begin{bmatrix} 0 \\ 1 \end{bmatrix}\begin{bmatrix} X \\ Y \end{bmatrix}\right\}, \tag{10}$$

where $X = x - x_c, Y = y - y_c$, (x_c, y_c) is the center of T.

Raviart-Thomas (RT) Spaces on Triangles

The Gram matrix of the basis functions is

$$GM = \begin{bmatrix} (\mathbf{w}_1, \mathbf{w}_1) & (\mathbf{w}_1, \mathbf{w}_2) & (\mathbf{w}_1, \mathbf{w}_3) \\ (\mathbf{w}_2, \mathbf{w}_1) & (\mathbf{w}_2, \mathbf{w}_2) & (\mathbf{w}_2, \mathbf{w}_3) \\ (\mathbf{w}_3, \mathbf{w}_1) & (\mathbf{w}_3, \mathbf{w}_2) & (\mathbf{w}_3, \mathbf{w}_3) \end{bmatrix} = \begin{bmatrix} |T| & 0 & 0 \\ 0 & |T| & 0 \\ 0 & 0 & S \end{bmatrix}, \quad (11)$$

where $|T|$ is the area of an triangle, and

$$S = \frac{|T|}{36}((x_1 - x_2)^2 + (x_2 - x_3)^2 + (x_3 - x_1)^2 + (y_1 - y_2)^2 + (y_2 - y_3)^2 + (y_3 - y_1)^2).$$

Raviart-Thomas (RT) Spaces on Triangles

Edge-based basis

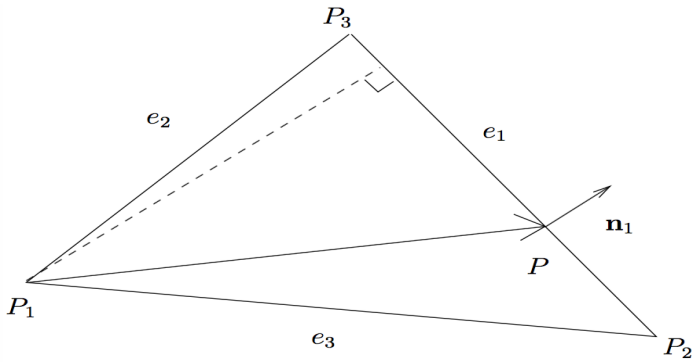

Figure: Edge-based basis for MFEMs

$$RT_0(T) = \text{Span}\{\phi_1,\ \phi_2,\ \phi_3\}, \tag{12}$$

and

$$\phi_1 = \frac{|e_1|}{2|T|}(P - P_1), \quad \phi_2 = \frac{|e_2|}{2|T|}(P - P_2), \quad \phi_3 = \frac{|e_3|}{2|T|}(P - P_3). \tag{13}$$

Two properties: $\phi_i \cdot n_j = \delta_{ij}$, $\nabla \cdot \phi_i = \frac{|e_i|}{|T|}$.

Features of MFEMs

- Satisfies local mass conservation,
- Satisfies bulk normal flux continuity,
- Need to satisfy the inf-sup condition,

$$\inf_{w\in\overline{W}_h, w\neq 0}\sup_{\mathbf{v}\in\overline{V}_h,\mathbf{v}\neq 0}\frac{(\nabla\cdot\mathbf{v}, w)}{\|\mathbf{v}\|_{H(div)}\|w\|_{L^2}} > 0,$$

- Results in indefinite discrete linear systems.

Weak Functions, Weak Gradients

Weak functions On an element E, the space of weak functions is

$$W(E) = \{v = \{v^\circ, v^\partial\}, v^\circ \in L^2(E), v^\partial \in L^2(E^\partial)\}. \quad (14)$$

Weak gradient $\nabla_w v$ is a functional defined through integration by parts,

$$(\nabla_w v, \mathbf{w}) = \int_{E^\partial} v^\partial(\mathbf{w} \cdot \mathbf{n}) - \int_E v^\circ(\nabla \cdot \mathbf{w}), \quad \mathbf{w} \in \mathrm{H}(\mathrm{div}, E). \quad (15)$$

A **discrete weak function** space on the element E is

$$W(E, l, m) = \{v = \{v^\circ, v^\partial\}, v^\circ \in P^l(E^\circ), v^\partial \in P^m(E^\partial)\}. \quad (16)$$

Two spaces of discrete weak functions on the mesh $\mathcal{E}_h$ are $S_h(l, m)$ and $S_h^0(l, m)$.

Discrete Weak Gradient

Discrete weak gradient is denoted as $\nabla_{w,d} v$, via integration by parts

$$\int_E (\nabla_{w,d} v) \cdot \mathbf{w} = \int_{E^\partial} v^\partial (\mathbf{w} \cdot \mathbf{n}) - \int_{E^\circ} v^\circ (\nabla \cdot \mathbf{w}), \ \mathbf{w} \in P^n(E)^2. \quad (17)$$

And $v^\circ \subset P^l(E^\circ)$, $v^\partial \subset P^m(E^\partial)$, $\nabla_{w,d} v \subset P^n(E)^2$.

On a triangular element T,

- $(P_0, P_0; RT_0)$, and $RT_0 \subset P^1(T)^2$;
- $(P_1, P_1; RT_1)$, and $RT_1 \subset P^2(T)^2$.

WG($P_0, P_0; RT_0$) Elements on Triangles

On each triangular element, there are four discrete weak functions: $\phi_0, \phi_1, \phi_2, \phi_3$,

- $\phi_0 = 1$ in the interior, $\phi_0 = 0$ on the three edges;
- $\phi_i = 1$ $(i = 1, 2, 3)$ on the very edge, $\phi_i = 0$ on the other edges and in the interior.

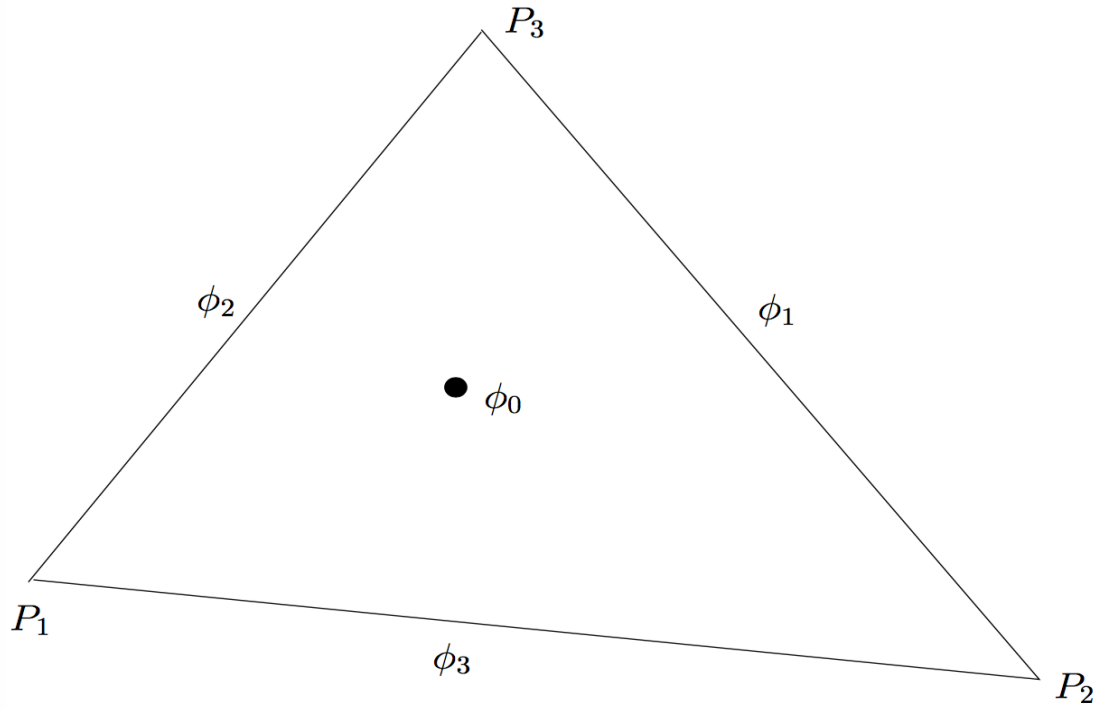

Figure: Weak functions on a triangle

WG($P_0, P_0; RT_0$) Elements on Triangles

Through integration by parts, we have a small SPD linear system,

$$\int_T (\nabla_{w,d}\phi)\cdot\mathbf{w} = \int_{T^\partial} \phi^\partial(\mathbf{w}\cdot\mathbf{n}) - \int_{T^\circ} \phi^\circ(\nabla\cdot\mathbf{w}),\ \forall \mathbf{w}\in RT_0(T). \tag{18}$$

And $\nabla_{w,d}\phi = \sum_{i=1}^{3} c_i\mathbf{w}_i$.

On each local element T, we have

$$\sum_{i=1}^{3} c_i \int_T \mathbf{w}_i\cdot\mathbf{w}_j = \int_{T^\partial} \phi^\partial(\mathbf{w}_j\cdot\mathbf{n}) - \int_{T^\circ} \phi^\circ(\nabla\cdot\mathbf{w}_j), \tag{19}$$

Discrete weak gradients of 4 basis functions are

$$\begin{cases} \nabla_{w,d}\phi_0 = 0\mathbf{w}_1 + 0\mathbf{w}_2 + \frac{-2|T|}{S}\mathbf{w}_3, \\ \nabla_{w,d}\phi_1 = \frac{(y_3-y_2)}{|T|}\mathbf{w}_1 + \frac{(x_2-x_3)}{|T|}\mathbf{w}_2 + \frac{2|T|}{3S}\mathbf{w}_3, \\ \nabla_{w,d}\phi_2 = \frac{(y_1-y_3)}{|T|}\mathbf{w}_1 + \frac{(x_3-x_1)}{|T|}\mathbf{w}_2 + \frac{2|T|}{3S}\mathbf{w}_3, \\ \nabla_{w,d}\phi_3 = \frac{(y_2-y_1)}{|T|}\mathbf{w}_1 + \frac{(x_1-x_2)}{|T|}\mathbf{w}_2 + \frac{2|T|}{3S}\mathbf{w}_3. \end{cases} \tag{20}$$

WG for Darcy: Pressure

Variational form of Darcy derived via integration by parts,
Seek $p \in H^1_{D,p_D}(\Omega)$, such that

$$\int_\Omega \mathbf{K}\nabla p \cdot \nabla q = \int_\Omega f\, q,\ q \in H^1_{D,0}(\Omega). \tag{21}$$

WG$(P_0, P_0; RT_0)$ scheme for the Darcy Equation
Seek $p_h = \{p_h^\circ, p_h^\partial\} \in S_h$ such that $p_h^\partial|_{\Gamma_h^D} = Q_h^\partial(p_D)$ and

$$\mathcal{A}_h(p_h, q) = \mathcal{F}(q), \qquad \forall q = \{q^\circ, q^\partial\} \in S_h^0, \tag{22}$$

where

$$\mathcal{A}_h(p_h, q) := \sum_{E\in\mathcal{E}_h} \int_E \mathbf{K}\nabla_{w,d} p_h \cdot \nabla_{w,d} q, \tag{23}$$

and

$$\mathcal{F}(q) := \sum_{E\in\mathcal{E}_h} \int_E f\, q^\circ \tag{24}$$

WG for Darcy: Pressure

$\nabla_{w,d} p_h = \sum_{i=0}^{3} a_i(\nabla_{w,d}\phi_i), \qquad \nabla_{w,d} q = \nabla_{w,d}\phi_j, (j = 0, 1, 2, 3).$

The finite element scheme on the whole mesh $\mathcal{T}_h$ is formulated as

$$\sum_{T\in\mathcal{T}_h}\int_T \mathbf{K}(\sum_{i=0}^{3} a_i(\nabla_{w,d}\phi_i))\cdot\nabla_{w,d}\phi_j = \sum_{T\in\mathcal{T}_h}\int_T f. \tag{25}$$

$$\sum_{T\in\mathcal{T}_h}\sum_{i=0}^{3}\int_T a_i(\mathbf{K}(\nabla_{w,d}\phi_i))\cdot\nabla_{w,d}\phi_j = \sum_{T\in\mathcal{T}_h}\int_T f. \tag{26}$$

The global stiffness matrix as a blocked matrix:

$$\begin{bmatrix} A_{ee} & A_{eg} \\ A_{ge} & A_{gg} \end{bmatrix}. \tag{27}$$

WG for Darcy: Velocity, Normal flux

Darcy Velocity

$$\mathbf{u}_h = -\mathbf{K}\nabla_{w,d} p_h, \tag{28}$$

If $\mathbf{K}\nabla_{w,d} p_h$ is not in Raviart-Thomas space, i.e., $\mathbf{K}$ is not diagonal, we use L_2-projection to project it to the space.

Bulk normal flux

$$\int_e \mathbf{u}_h \cdot \mathbf{n} = \mathbf{u}_h \cdot \mathbf{n}|e|, \tag{29}$$

where $\mathbf{u}_h$ is the numerical velocity at the edge's midpoint, $\mathbf{n}$ is the outward unit vector, $|e|$ is the edge length.

Properties of the Lowest-order WG Scheme

Local mass conservation

$$\int_E f = \int_{E^\partial} \mathbf{u}_h \cdot \mathbf{n}.$$

Proof. Take a test function q so that $q|_{E^\circ} = 1$ but vanishes on all edges and inside all other elements. Then

$$\begin{aligned}
\int_E f &= \int_E (\mathbf{K}\nabla_{w,d} p_h) \cdot \nabla_{w,d} q = \int_E \mathbf{Q}_h(\mathbf{K}\nabla_{w,d} p_h) \cdot \nabla_{w,d} q \\
&= -\int_E \mathbf{u}_h \cdot \nabla_{w,d} q = -\int_{E^\partial} q^\partial (\mathbf{u}_h \cdot \mathbf{n}) + \int_{E^\circ} q^\circ (\nabla \cdot \mathbf{u}_h) \\
&= \int_{E^\circ} \nabla \cdot \mathbf{u}_h = \int_{E^\partial} \mathbf{u}_h \cdot \mathbf{n}.
\end{aligned}$$

Continuity of bulk normal fluxes

If $\partial E_1 \cap \partial E_2 = \gamma$, $\mathbf{n_1}, \mathbf{n_2}$ are the constant outward unit vectors on γ, there holds

$$\int_\gamma \mathbf{u}_h^{(1)} \cdot \mathbf{n}_1 + \int_\gamma \mathbf{u}_h^{(2)} \cdot \mathbf{n}_2 = 0.$$

Proof. We take a test function $q = \{q^\circ, q^\partial\}$ such that $q^\partial = 1$ only on the very edge γ; but $q^\partial = 0$ on all other edges and $q^\circ = 0$ in interior of any quadrilateral or triangular element. We have

$$\begin{aligned}
0 &= \int_{E_1} (\mathbf{K}\nabla_{w,d} p_h) \cdot \nabla_{w,d} q + \int_{E_2} (\mathbf{K}\nabla_{w,d} p_h) \cdot \nabla_{w,d} q \\
&= \int_{E_1} \mathbf{Q}_h(\mathbf{K}\nabla_{w,d} p_h) \cdot \nabla_{w,d} q + \int_{E_2} \mathbf{Q}_h(\mathbf{K}\nabla_{w,d} p_h) \cdot \nabla_{w,d} q \\
&= \int_{E_1} (-\mathbf{u}_h^{(1)}) \cdot \nabla_{w,d} q + \int_{E_2} (-\mathbf{u}_h^{(2)}) \cdot \nabla_{w,d} q \\
&= -\int_\gamma \mathbf{u}_h^{(1)} \cdot \mathbf{n}_1 - \int_\gamma \mathbf{u}_h^{(2)} \cdot \mathbf{n}_2.
\end{aligned}$$

Convergence in Pressure, Velocity and Flux

L^2-norms:

$$\|p - p_h^\circ\|^2 = \sum_{E \in \mathcal{E}_h} \|p - p_h^\circ\|^2_{L^2(E)}, \tag{30}$$

$$\|\mathbf{u} - \mathbf{u}_h\|^2 = \sum_{E \in \mathcal{E}_h} \|\mathbf{u} - \mathbf{u}_h\|^2_{L^2(E)^2}, \tag{31}$$

$$\|(\mathbf{u} - \mathbf{u}_h) \cdot \mathbf{n}\|^2 = \sum_{E \in \mathcal{E}_h} \sum_{\gamma \subset E^\partial} \frac{|E|}{|\gamma|} \|\mathbf{u} \cdot \mathbf{n} - \mathbf{u}_h \cdot \mathbf{n}\|^2_{L^2(\gamma)}. \tag{32}$$

Proposition

Let p be the exact solution of the Darcy problem and $\mathbf{u} = -\mathbf{K}\nabla p$. Assume the exact solution has regularity $p \in H^{1+s}(\Omega)$ and $\mathbf{u} \in H^s(\Omega)^2$ for some $s \in (0, 1]$. When the quadrilaterals are asymptotically parallelograms, there holds

$$\|p - p_h^\circ\| \leq Ch, \quad \|\mathbf{u} - \mathbf{u}_h\| \leq Ch^s, \quad \|(\mathbf{u} - \mathbf{u}_h) \cdot \mathbf{n}\| \leq Ch^s, \tag{33}$$

where $C > 0$ is a constant that is independent of the mesh size h.

WG Finite Elements on Quadrilaterals

On each quadrilateral element, local Raviart-Thomas space

$$RT_{[0]} = \text{Span}(\mathbf{w}_1, \mathbf{w}_2, \mathbf{w}_3, \mathbf{w}_4),$$

with $\mathbf{w}_1 = \begin{bmatrix} 1 \\ 0 \end{bmatrix}$, $\mathbf{w}_2 = \begin{bmatrix} 0 \\ 1 \end{bmatrix}$, $\mathbf{w}_3 = \begin{bmatrix} X \\ 0 \end{bmatrix}$, $\mathbf{w}_4 = \begin{bmatrix} 0 \\ Y \end{bmatrix}$.

$$GM = [< \mathbf{w}_i, \mathbf{w}_j >] = \begin{bmatrix} |E| & 0 & \int_E X & 0 \\ 0 & |E| & 0 & \int_E Y \\ \int_E X & 0 & \int_E X^2 & 0 \\ 0 & \int_E Y & 0 & \int_E Y^2 \end{bmatrix}. \tag{34}$$

When E is a rectangle, the Gram matrix becomes a diagonal matrix, with $\int_E X$ and $\int_E Y = 0$.

Quadrilateral and Hybrid Meshes

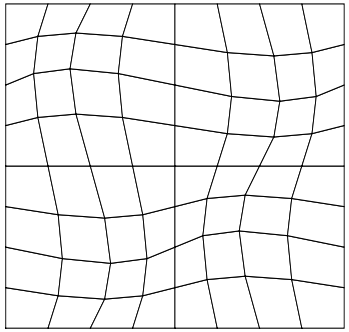

Type I

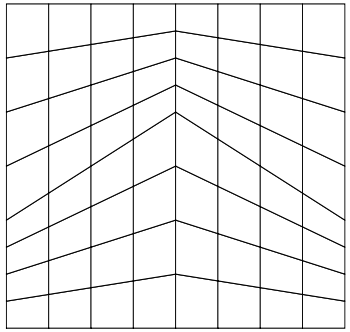

Type II

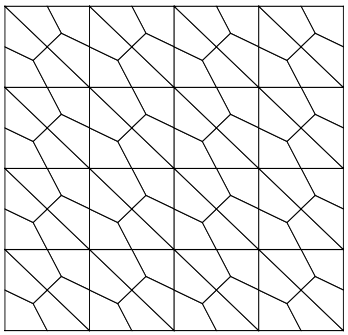

Type III

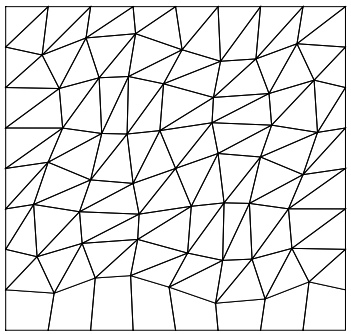

Type IV

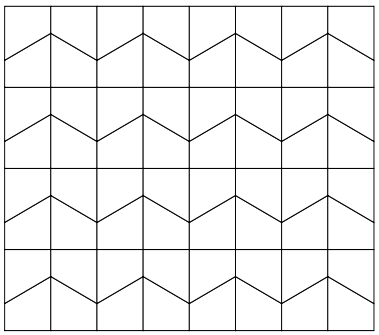

Type V

Figure: Four types of meshes for numerical experiments. Type I: Whee, Xue, Yotov, *Numer. Math.* (2012), Type II: Arnold, Boffi, Falk, *Math. Comput.* (2002), Type III, Type IV: Liu, Tavener, Wang, (Submitted).

Example 1: Smooth Solution, 1st. Order Convergence

$\Omega = (0,1)^2, \mathbf{K} = \mathbf{I}_2$. Analytical solution:
$p(x,y) = \sin^2(\pi x)\sin(\pi y)$, and a homogeneous Dirichlet boundary condition on the entire boundary, $f(x,y) = 2\pi^2 \sin(\pi x)\sin(\pi y)$.

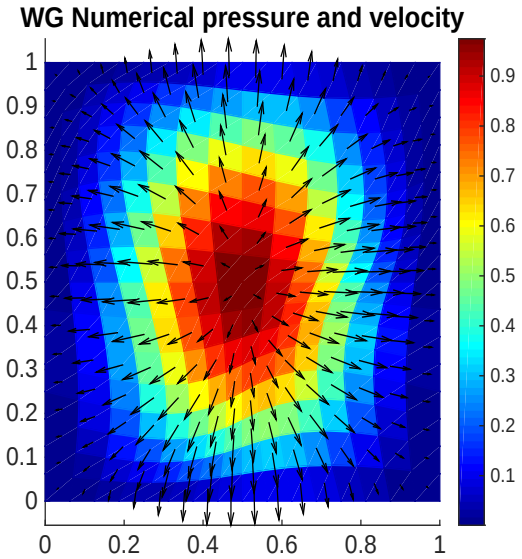

Type I mesh

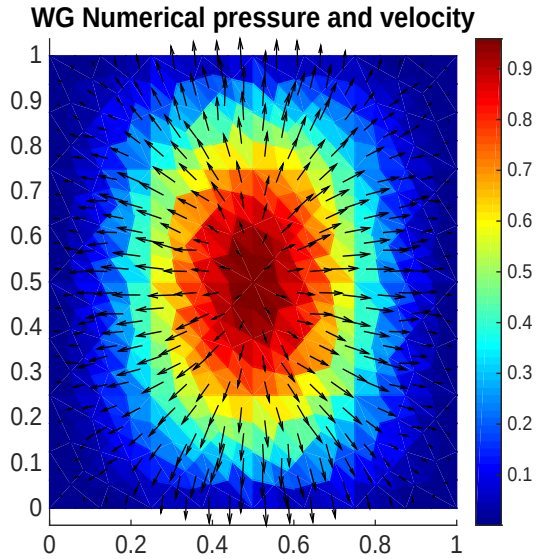

Type III mesh

Figure: Example 1: Profiles of numerical pressure and velocity from the weak Galerkin method on a logically rectangular mesh (left) and a quadrilateral mesh (right). Both have mesh size $h = 1/16$.

Example 1: Smooth Solution, 1st. Order Convergence

Table: Smooth solution example: Numerical results of WG($Q_0, Q_0; RT_{[0]}$) method on quadrilateral meshes

$1/h$	$\|p - p_h^\circ\|$	$\|\mathbf{u} - \mathbf{u}_h\|$	$\|(\mathbf{u} - \mathbf{u}_h) \cdot \mathbf{n}\|$	$\min(p_h^\circ)$	$\max(p_h^\circ)$
Type I meshes					
8	7.9787e-02	2.9333e-01	3.9052e-01	4.9321e-03	9.1103e-01
16	3.9992e-02	1.4134e-01	1.9217e-01	7.9909e-04	9.7451e-01
32	2.0008e-02	6.9866e-02	9.5649e-02	1.2073e-04	9.9313e-01
64	1.0006e-02	3.4827e-02	4.7769e-02	1.6882e-05	9.9822e-01
Conv.rate	0.998	1.024	1.01	N/A	N/A
Type III meshes					
8	7.8950e-02	7.1381e-01	9.2420e-01	-5.4381e-03	8.6684e-01
16	3.6052e-02	3.5510e-01	4.6914e-01	9.1560e-04	9.5896e-01
32	1.7429e-02	1.6021e-01	2.1262e-01	1.4879e-04	9.9110e-01
64	8.6739e-03	7.3582e-02	9.8494e-02	2.0641e-05	9.9823e-01
Conv.rate	1.062	1.092	1.076	N/A	N/A

Example 2: Low Regularity, $a = \frac{1}{3}$

$\Omega = (0,1)^2$, $\mathbf{K} = \mathbf{I}_2$, a homogeneous Dirichlet boundary condition on the entire boundary, and an analytical solution, where $a \in (0,1]$ is a regularity parameter,

$$p(x,y) = x(1-x)y(1-y)\left(\sqrt{x^2+y^2}\right)^{-(2-a)}.$$

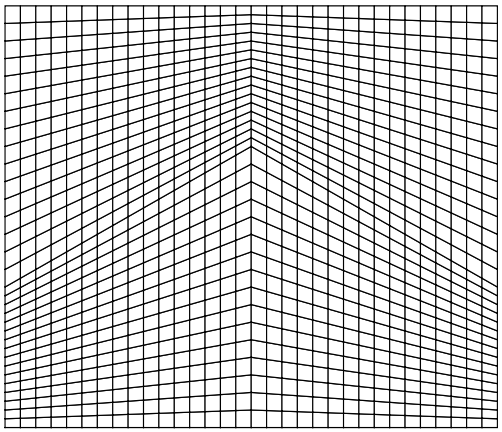

Type II mesh

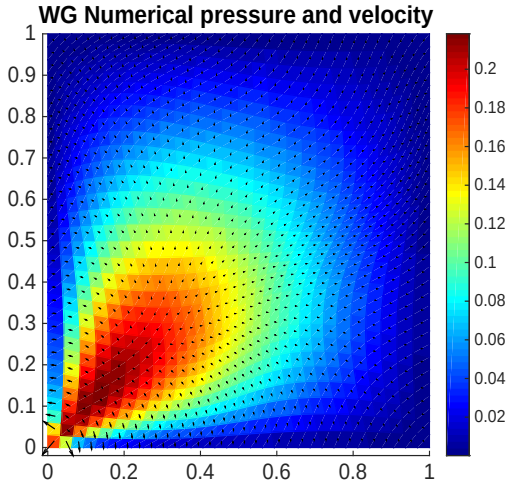

Numerical results

Figure: Lower regularity: Numerical pressure and velocity from the lowest-order weak Galerkin method on an asymptotically parallelogram mesh with mesh size $h = 1/32$.

Example 2: Low Regularity, $a = \frac{1}{3}$

Table: Example: Numerical results of WG($Q_0, Q_0; RT_{[0]}$) method on asymptotically parallelogram quadrilateral meshes

$1/h$	$\|p - p_h^\circ\|$	$\|\mathbf{u} - \mathbf{u}_h\|$	$\|(\mathbf{u} - \mathbf{u}_h) \cdot \mathbf{n}\|$	$\min(p_h^\circ)$	$\max(p_h^\circ)$
8	2.67E-02	5.0765E-01	1.6957E+00	2.5994E-03	2.6493E-01
16	1.2341E-02	3.9273E-01	1.3020E+00	6.7727E-04	2.3842E-01
32	5.9880E-03	3.0796E-01	1.0164E+00	1.7388E-04	2.1801E-01
64	2.9648E-03	2.4305E-01	8.0019E-01	4.2116E-05	2.1582E-01
128	1.4782E-03	1.9239E-01	6.3256E-01	1.0354E-05	2.1564E-01
Conv.rate	1.043	0.349	0.355	N/A	N/A

Example 3: WGFEMs on Hybrid Meshes

The exact solution for the pressure is $p = \sin(\pi x)\sin(\pi y)$. On the domain $\Omega = (0,1)^2$, $\mathbf{K} = \mathbf{I}_2$ and a homogeneous Dirichlet boundary condition on the entire boundary.

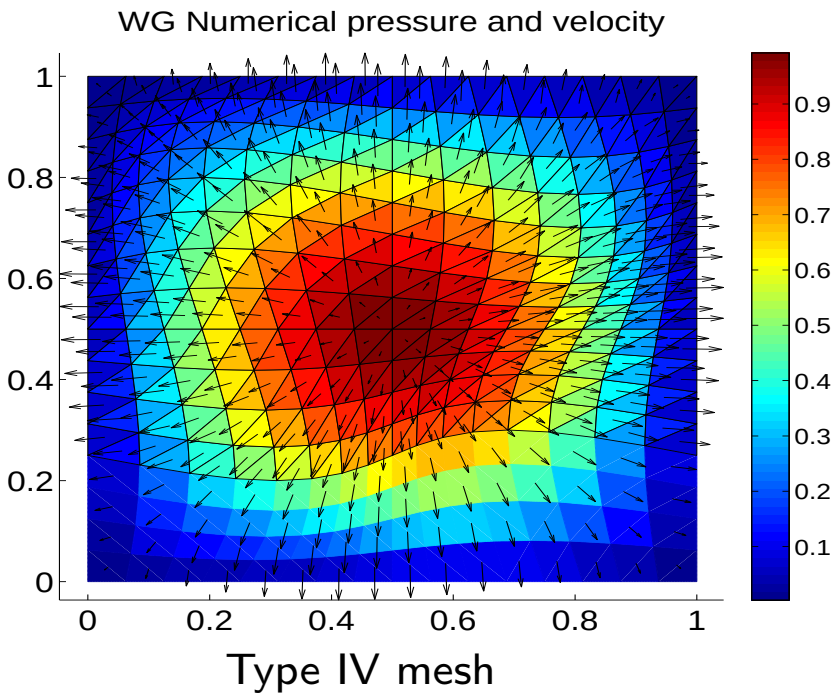

Figure: *N*umerical pressure and velocity from WGFEMs on a hybrid mesh with mesh size $h = 1/16$. Liu, Tavener, Wang, (Submitted).

Example 3: WGFEMs on Hybrid Meshes

Table: Example: Numerical results of WG($Q_0, Q_0; RT_{[0]}$) method on hybrid meshes, results from Liu, Tavener, Wang, (Submitted).

$1/h$	$\|p - p_h^\circ\|$	$\|\mathbf{u} - \mathbf{u}_h\|$	$\|(\mathbf{u} - \mathbf{u}_h) \cdot \mathbf{n}\|$	$\min(p_h^\circ)$	$\max(p_h^\circ)$
8	7.2665e-2	2.7675e-1	3.3213e-1	1.3150e-2	9.6983e-1
16	3.6563e-2	1.3839e-1	1.6405e-1	3.3015e-3	9.9233e-1
32	1.8311e-2	6.9195e-2	8.1719e-2	8.1269e-4	9.9807e-1
64	9.1592e-3	3.4598e-2	4.0817e-2	2.0159e-4	9.9952e-1
Conv.rate	0.995	0.999	1.008	N/A	N/A

WG $(Q_0, Q_0; RT_{[0]})$ Elements on Hexahedra

On a hexahedron E, the local Raviart-Thomas space is defined as

$$RT_{[0]}(E) = \text{Span}(\mathbf{w}_1, \mathbf{w}_2, \mathbf{w}_3, \mathbf{w}_4, \mathbf{w}_5, \mathbf{w}_6). \tag{35}$$

$$\mathbf{w}_1 = \begin{bmatrix} 1 \\ 0 \\ 0 \end{bmatrix}, \mathbf{w}_2 = \begin{bmatrix} 0 \\ 1 \\ 0 \end{bmatrix}, \mathbf{w}_3 = \begin{bmatrix} 0 \\ 0 \\ 1 \end{bmatrix},$$

$$\mathbf{w}_4 = \begin{bmatrix} X \\ 0 \\ 0 \end{bmatrix}, \mathbf{w}_5 = \begin{bmatrix} 0 \\ Y \\ 0 \end{bmatrix}, \mathbf{w}_6 = \begin{bmatrix} 0 \\ 0 \\ Z \end{bmatrix}.$$

Discrete weak functions. $\phi_0, \phi_1, \phi_2, \phi_3, \phi_4, \phi_5, \phi_6.$

Example 4: Smooth Solution, 1st. Order Convergence

$\Omega = (0,1)^3$ (the unit cube) with the exact solution values on Dirichlet boundary, $\mathbf{K} = \mathbf{I}_3$. Analytic solution:
$p(x,y,z) = \cos(\pi x)\cos(\pi y)\cos(\pi z)$.

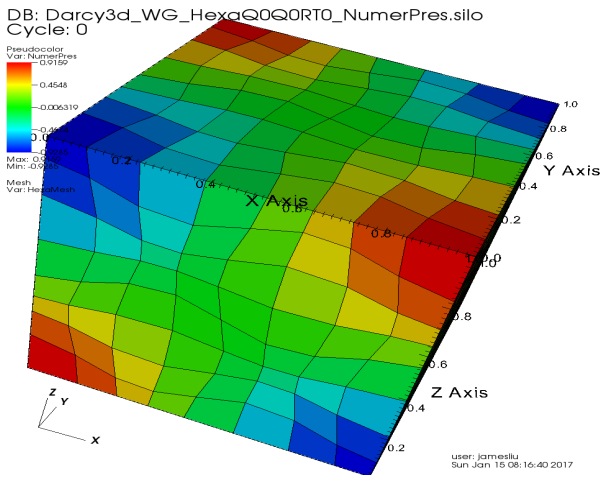

Hexahedral meshes Type I, $h = 1/8$

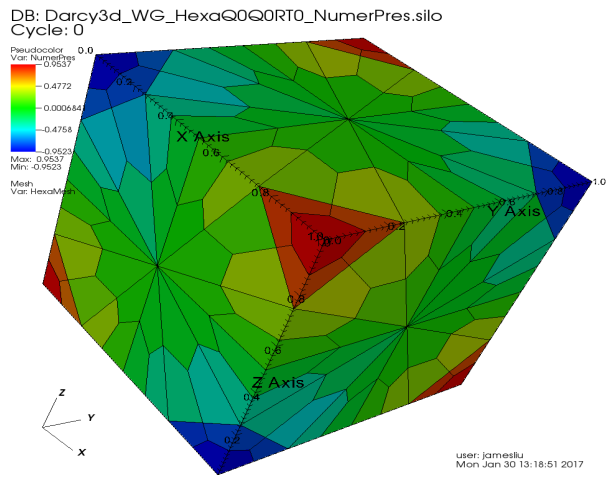

Hexahedral meshes Type II , $h = 1/8$

Figure: Example 4: Numerical pressure profiles on two hexahedral meshes. Harper, Liu, Zheng, *Numer. Math.* (2017).

Example 4: Smooth Solution, 1st. Order Convergence

Table: Example 4: Convergence rates of errors in pressure, velocity, and flux on the logically brick meshes. Harper, Liu, Zheng, *Numer. Math.* (2017).

1/h	$\|p - p_h^\circ\|$	$\|\mathbf{u} - \mathbf{u}_h\|$	$\|(\mathbf{u} - \mathbf{u}_h) \cdot \mathbf{n}\|$
8	7.0011E-2	3.2844E-1	7.1386E-2
16	3.5623E-2	1.6527E-1	3.5469E-2
32	1.7905E-2	8.2288E-2	1.7623E-2
64	8.9652E-3	4.1069E-2	8.7969E-3
Conv.rate	0.988	0.999	1.006

Table: Example 4: Convergence rates of errors in pressure, velocity, and flux on the hexahedral meshes Harper, Liu, Zheng, *Numer. Math.* (2017).

1/h	$\|p - p_h^\circ\|$	$\|\mathbf{u} - \mathbf{u}_h\|$	$\|(\mathbf{u} - \mathbf{u}_h) \cdot \mathbf{n}\|$
4	3.0310E-5	1.2359E-3	2.2008E-4
8	1.4466E-5	5.7003E-4	1.2107E-4
16	7.1904E-6	2.8141E-4	6.2760E-5
32	3.6280E-6	1.4303E-4	3.2173E-5
64	1.8858E-6	7.7412E-5	1.7172E-5
Conv.rate	1.001	0.998	0.920

WGFEMs for Elasticity (Work in Progress)

$$\begin{cases} -\nabla \cdot \sigma(\mathbf{u}) = \mathbf{f}, & \text{in } \Omega, \\ \mathbf{u} = \hat{\mathbf{u}}, & \text{on } \Gamma, \end{cases} \tag{36}$$

- $\mathbf{u}$ is the displacement vector
- $\mathbf{f}$ is the exterior force
- $\hat{\mathbf{u}}$ is boundary value
- $\varepsilon(\mathbf{u})$ is the strain tensor, $\varepsilon(\mathbf{u}) = \frac{1}{2}(\nabla \mathbf{u} + \nabla(\mathbf{u})^T)$
- $\sigma(\mathbf{u})$ is the stress tensor, $\sigma(\mathbf{u}) = 2\mu\varepsilon(\mathbf{u}) + \lambda(\nabla \cdot \mathbf{u})\mathbf{I}$
- λ and μ are Lamé constants

Discrete Weak Divergence, Discrete Weak Divergence

Weak divergence is a linear functional in $H^1(E)$, denoted as $\nabla_w \cdot \mathbf{v}$,

$$\int_E (\nabla_w \cdot \mathbf{v})\phi = -\int_{E^\circ} \mathbf{v}^\circ \cdot (\nabla\phi) + \int_{E^\partial} \mathbf{v}^\partial \cdot (\phi\, \mathbf{n}), \tag{37}$$

Discrete weak divergence is denoted as $\nabla_{w,d} \cdot \mathbf{v} \in P^r(E)$,

$$\int_E (\nabla_{w,d} \cdot \mathbf{v})\phi = -\int_{E^\circ} \mathbf{v}^\circ \cdot (\nabla\phi) + \int_{E^\partial} \mathbf{v}^\partial \cdot (\phi\, \mathbf{n}), \quad \forall \phi \in P^r(E) \tag{38}$$

Discrete Weak Gradient

Weak gradient is a linear functional in the Soblev space $H^1(E)^{2\times 2}$, and denoted as $\nabla_w \mathbf{v}$,

$$\int_E (\nabla_w \mathbf{v}) : W = -\int_{E^\circ} \mathbf{v}^\circ \cdot (\nabla \cdot W) + \int_{E^\partial} \mathbf{v}^\partial \cdot (W\mathbf{n}), \quad \forall W \in H^1(E)^{2\times 2}, \tag{39}$$

where W is a 2×2 matrix with entries in $H^1(E)$, $\mathbf{n}$ is the outward normal vectors on E^∂.

Discrete weak gradient $\nabla_{w,d}\mathbf{v}$ is a matrix valued polynomial,

$$\int_E (\nabla_{w,d} \mathbf{v}) : W = -\int_{E^\circ} \mathbf{v}^\circ \cdot (\nabla \cdot W) + \int_{E^\partial} \mathbf{v}^\partial \cdot (W\mathbf{n}), \quad \forall W \in P^r(E)^{2\times 2}, \tag{40}$$

where W is a matrix-valued degree r polynomial.

WG(Q_0^2, Q_0^2; $RT_{[0]}^2$, Q_0) FE Scheme

Space of discrete weak function E is

$$W(E, l, m) = \{\mathbf{v} = (\mathbf{v}^\circ, \mathbf{v}^\partial), \mathbf{v}^\circ \in P^l(E^\circ)^2, \mathbf{v}^\partial \in P^m(E^\partial)^2\}. \quad (41)$$

Spaces of discrete weak functions over $\mathcal{E}_h$ are S_h and S_h^0.

Find $\mathbf{u}_h = \{\mathbf{u}_h^\circ, \mathbf{u}_h^\partial\} \in S_h$, and $\mathbf{u}_h^\partial|_{\Gamma_h} = Q_h^\partial(\mathbf{u}_D)$, such that

$$\mathcal{A}(\mathbf{u}_h, \mathbf{v}) = \mathcal{F}(\mathbf{v}), \quad \forall \mathbf{v} \in S_h^0, \quad (42)$$

where

$$\mathcal{A}(\mathbf{u}_h, \mathbf{v}) = \sum_{E \in \mathcal{E}_h} 2\mu(\varepsilon_{w,d}(\mathbf{u}_h), \varepsilon_{w,d}(\mathbf{v}))_E + \sum_{E \in \mathcal{E}_h} \lambda(\nabla_{w,d} \cdot \mathbf{u}_h, \nabla_{w,d} \cdot \mathbf{v})_E, \quad (43)$$

$$\mathcal{F}(\mathbf{v}) = \sum_{E \in \mathcal{E}_h} (\mathbf{f}, \mathbf{v})_E. \quad (44)$$

Summary: Nice Features of WGFEMs for Darcy Equation

The advantages of lowest order WG method:

- easy just constants
- generality: work for
  - purely trig. mesh
  - purely rect. mesh
  - purely quadri. mesh
    (rect. mesh becomes a special case of quadri. mesh)
  - a mix of any above
  - 3-dim.

SPD global lin. sys. compared to infinite lin. sys. from mixed methds.

Two important physical properties expected convergence.

G. Harper, J. Liu, and B. Zheng.
The THex algorithm and a simple Darcy solver on hexahedral meshes.
Proc. Comput. Sci., pages Preprint, Colorado Sate University, 2017.

J. Liu, S. Tavener, and Z. Wang.
The lowest-order weak galerkin finite element method for the darcy equation on quadrilateral and hybrid meshes.
Submitted.

M. Wheeler, G. Xue, and I. Yotov.
A multipoint flux mixed finite element method on distorted quadrilaterals and hexahedra.
Numer. Math., 2012.